

# Inverse resistivity problem: geoelectric uncertainty principle and numerical reconstruction method

BALGAYSHA MUKANOVA<sup>1</sup> and MURAT ORUNKHANOV<sup>2</sup>

*The Faculty of Mechanics and Mathematics  
Al-Farabi Kazakh National University  
Almaty-505012, Masanchi str. 39/47  
KAZAKHSTAN*

**Abstract.** Mathematical model of vertical electrical sounding by using resistivity method is studied. The model leads to an inverse problem of determination of the unknown leading coefficient (conductivity) of the elliptic equation in  $R^2$  in a slab. The direct problem is obtained in the form of mixed BVP in axisymmetric cylindrical coordinates. The additional (available measured) data is given on the upper boundary of the slab, in the form of tangential derivative. Due to ill-conditionedness of the considered inverse problem the logarithmic transformation is applied to the unknown coefficient and the inverse problem is studied as a minimization problem for the cost functional, with respect to the reflection coefficient. The Conjugate Gradient (CGM) method is applied for the numerical solution of this problem. Computational experiments were performed with noise free and random noisy data.

**Key words:** inverse problem, resistivity reconstruction, uncertainty principle, numerical solution

**AMS(MOS) subject classifications** 34A55, 35R30, 65L08

## 1. Introduction

Construction of nondestructive control technologies and determination of material parameters always play an essential practical and theoretical interests (see, [4,11-14, 17] and references therein). Concerning to mineral exploration, this is an interpretation problem of surface or near-surface prospecting. One of the popular methods of exploration is the vertical electric sounding (VES) [11,12]. The main distinguished feature of this method is that it may provide the larger depth, and it is the most convenient for computer realization.

The problem related to the medium response with respect to electromagnetic field perturbation goes back to 1930s, in particular to the works of Slihter [20], Stefanescu and Shlumberger [21], Stevenson [22], A.N.Tikhonov [23-25]. The main scope of these initial works were limited to simple models of medium. Specifically, horizontally layered medium, local inclusion of the spherical form, an inclined layer and vertical contact.

We consider the following inverse coefficient problem: Find the function  $\sigma(z)$  via the solution of the boundary value problem

$$\left\{ \begin{array}{l} \frac{\partial}{\partial z} (\sigma(z) \frac{\partial u}{\partial z}) + \frac{\sigma(z)}{r} \frac{\partial}{\partial r} (r \frac{\partial u}{\partial r}) = 0, \quad (r, z) \in \Omega \subset R^2, \\ \sigma(0) \frac{\partial u}{\partial z} |_{z=0} = \delta(r), \\ u(r, z) |_{z=H} = 0, \\ \lim_{r \rightarrow \infty} u(r, z) = 0 \end{array} \right. \quad (1)$$

from the measured data  $\psi(r)$  defined as

$$\frac{\partial u}{\partial r} |_{z=0} = \psi(r). \quad (2)$$

---

<sup>1</sup>Corresponding author. *E-mail address:* mbsha01@gmail.com (B.Mukanova)

<sup>2</sup>*E-mail* : Murat.Orunhanov@kaznu.kz (M. Orunhanov)

Here  $\Omega = \{(r, z) \in R^2 : 0 \leq r < \infty, 0 < z < H\}$ . The function  $\sigma(z)$  satisfies the following conditions:  $\sigma(z) \in C[0, H] \cap C^2(0, H)$  and  $\sigma_2 \geq \sigma(z) \geq \sigma_1 > 0$ . The boundary condition at  $z = H$  is the approximation of the limiting value at the infinity. The additional condition (2) has the form of the tangential derivative of the potential  $u(r, z)$ , which is rather realistic for measured data [1,9-11]. The problem (1)-(2) will be defined as a *VES-inverse problem*. Correspondingly, the boundary value problem (1) will be defined as a *direct (or forward) problem*. The function  $\psi(r)$  is defined to be the *measured output data*, and function  $\sigma(z)$  is defined to be the *input data* [7-8].

Similar mathematical models related to inverse conductivity problems for finite dimensional bodies have been considered by many authors (see, for instance, [4, 19] and references therein). In the case of nearly constant conductivity coefficient a method of determination with geophysical applications have been given in [3], by using the Dirichlet-to-Neumann mapping. In all these studies the domain  $\Omega$  is assumed to be a bounded one. The considered here inverse problem can also be considered as a continuation of the study started in [1]. Here the domain  $\Omega$  has the form of a slab and the direct problem represents a mixed elliptic problem. In addition, on the upper boundary  $z = 0$  the source term is given in the form of a pointwise flux.

Let  $u = u(r, z; \sigma)$  be the unique solution of the direct problem (1) for a given coefficient  $\sigma(z) \in \mathcal{S}$ , where  $\mathcal{S} \subset C^2(0, H) \cap C[0, H]$  is the set of admissible coefficients which will be defined below. Further, we introduce the trace operator

$$\Lambda[\sigma] := \frac{\partial u(r, z; \sigma)}{\partial r} \Big|_{z=0}. \quad (3)$$

In view of this definition above inverse problem can be formulated in the following operator form:

$$\Lambda[\sigma](r) = \psi(r), \quad r \in [0, \infty). \quad (4)$$

Therefore the inverse problem (1)-(2) with the given measured output data  $\psi(r)$  can be reduced to the solution of the nonlinear equation (4) or to inverting the coefficient-data (or input-output) map  $\Lambda : \mathcal{S} \mapsto \Psi$ , where  $\Psi$  is the set of measured data which will be defined below. Note that the main uniqueness result for this problem has been obtained by Tikhonov in [24]. Namely, if  $\sigma(z), \tilde{\sigma}(z) \in \mathcal{S}$  and  $\Lambda[\sigma] = \Lambda[\tilde{\sigma}]$ , then  $\sigma(z) \equiv \tilde{\sigma}$ .

Due to measurements errors the inverse problem (4) may not have a solution in any suitable class of admissible coefficients. For this reason we introduce the following auxiliary (cost) functional

$$J(\sigma) = \int_0^\infty [\Lambda[\sigma](r) - \psi(r)]^2 r dr, \quad \sigma \in \mathcal{S}, \quad (5)$$

according to [27], and consider the following minimization problem:

$$J(\sigma_*) = \inf J(\sigma), \quad \sigma \in \mathcal{S}.$$

Due to the physical meaning of the problem the source term has the form of the Dirac Delta function, and the above form of the functional  $J(\sigma)$  is not convenient for numerical implementation. On the other hand, the unknown coefficient  $\sigma(z)$  depends only on the variable  $z \in [0, H]$ . This permits one to apply Bessel transformation with respect to the variable  $r \in [0, \infty)$ . As a result the direct problem is reduced to the boundary value problem for the second order ordinary differential equation, which can easily be solved by any standard method.

Since a direct problem is a part of the inverse problem, one needs, first of all, to construct an effective algorithm for the numerical solution of the direct problem. For the case of simple layered medium an analytical solution of the considered above direct problem (1) has been given in [9, 11, 26]. Further, for simplest cases when conductivity functions  $\sigma(z)$  has the form horst, ledge or graben, numerical solutions of the direct problem have been given in [12]. Some numerical results obtained in [17] for two-dimensional inverse problem are based on synthetic output data. Specifically, a database

for the output data here is based on numerical solutions of the corresponding forward problem for various input parameters.

The paper is organized as follows. Bessel-Fourier transformation of the direct problem and the auxiliary functional is derived in Section 2. This section contains also formula for the gradient of the transformed auxiliary functional. Results of computational experiments with noise free and noisy data are derived in the final Section 3. In Appendix we describe an influence of the reflection coefficient to the output data.

## 2. Bessel-Fourier transformation and gradient of the cost functional in terms of reflection coefficient

For the numerical solution of the considered inverse problem (1)-(2) we will use the gradient method [2,28]. For this aim we first need to derive the gradient of the auxiliary functional.

Note that in existing literature [see, for example,[1],[11], [18],[19]], numerical methods are based on the direct reconstruction of the unknown conductivity or resistivity coefficient. This leads to well-known difficulties. For example, in [1] authors use the smoothing procedure for  $\sigma(z)$  at each iteration. The main distinguished feature of the presented here approach is that the reflection factor is recovered at the first step. For this aim the inverse problem (1)-(2), as well as the auxiliary functional, are reformulated by using Bessel-Fourier transformation. Then the gradient  $\nabla J[p]$  of the cost functional (5) is derived in terms of the transformed reflection coefficient  $p(z)$ . This function will be defined also as a reflection factor function, due to its physical meaning.

To define the reflection factor function  $p(z)$ , let us first introduce the uniform grid  $w_h = \{z_i \in [0, H] : z_i = ih, h = H/N_z, i = \overline{0, N_z}\}$ , with the grid step  $h > 0$ , and consider an analogue of this function at the grid point  $z_i \in w_h$ . This analogue can be defined via the discrete values  $\sigma_i = \sigma(z_i)$  of the conductivity  $\sigma(z)$ , according to the definition of the reflection coefficient (or reflection factor)  $\mu$ , defined as  $\mu = (\sigma_1 - \sigma_2)/(\sigma_1 + \sigma_2)$ , at the transmission boundary between the inclusion and the surrounding medium (see, Appendix). Thus, the reflection factor  $\mu_i$  at grid point  $z_i \in w_h$  can be defined as follows:  $\mu_i = (\sigma_i - \sigma_{i+1})/(\sigma_i + \sigma_{i+1})$ . Since  $\sigma_i - \sigma_{i+1} = -h\sigma'_{i+1/2} + O(h^2)$ ,  $(\sigma_i + \sigma_{i+1})/2 = \sigma_{i+1/2} + O(h^2)$ , we have

$$\mu_i = -\frac{h\sigma'_{i+1/2}}{2\sigma_{i+1/2}} + O(h^2) = -\frac{1}{2} \int_i^{i+1} (\ln \sigma(z))' dz + O(h^2).$$

Therefore the discrete analogue of the reflection factor at grid point  $z_i \in w_h$  can approximately be defined as follows:

$$\mu_i \approx -\frac{(\ln \sigma_{i+1/2})'}{2}. \quad (6)$$

Formula (6) (see also explanation given in Appendix) suggests that the function  $p(z) = (\ln(\sigma(z)))'$  can be defined as the reflection factor function, and the inverse resistivity problem can be reformulated in terms of this function. Evidently, the conductivity function  $\sigma(z)$  can be defined via the reflection factor function  $p(z)$  as follow:

$$\sigma(z) = \sigma(0) \exp \left( \int_0^z p(z) dz \right). \quad (7)$$

Below we will use the following representation of the solution  $u(r, z)$  of problem (1)-(2) (see [23]), which has the singularity at the point  $(0,0)$ :

$$u(r, z) = -\frac{1}{\sigma(0)\sqrt{r^2 + z^2}} + \bar{u}(r, z), \quad \bar{u}(r, z) = O(\sqrt{r^2 + z^2}^{-1}), \quad r, z \rightarrow \infty. \quad (8)$$

Evidently,  $\bar{u}(r, z)$  is a bounded and regular at infinity function. The first term of the right hand side of (8) is the potential of the pointwise source. The current density for the pointwise source can be modelled by the delta function  $\delta(r)$ , given in (1). As a result, the function  $\bar{u}(r, z)$  satisfies the homogeneous flux boundary condition:

$$\sigma(0) \frac{\partial \bar{u}}{\partial z} \Big|_{z=0} = 0.$$

Let us define the set of measured data as follow:

$$\Psi = \{ \psi(r) | \psi(r) = \frac{1}{\sigma(0)r^2} + \bar{\psi}(r), \int_0^\infty |\bar{\psi}(r)| \sqrt{r} dr < \infty, 0 < r < \infty \}. \quad (9)$$

As it was mentioned above, we will use the Bessel-Fourier transformation with respect to the variable  $r \geq 0$ . For this aim let us denote by  $V(\lambda, z)$  the image of the function  $u(r, z)$ . Using (8) and Lipschitz integral formula we get

$$V(\lambda, z) = \int_0^\infty u(r, z) J_0(\lambda r) r dr = -\frac{e^{-\lambda z}}{\sigma(0)\lambda} + \int_0^\infty \bar{u}(r, z) J_0(\lambda r) r dr. \quad (10)$$

Hence,

$$V(\lambda, z) = -\frac{e^{-\lambda z}}{\sigma(0)\lambda} + \bar{V}(\lambda, z). \quad (11)$$

It was shown in [24] that the last integral in the formula (10) exists and converges uniformly. Further, it was established also that the function  $V(\lambda, z)$  satisfies the parameter-dependent ordinary differential equation

$$\frac{d}{dz} \left[ \sigma(z) \frac{dV}{dz} \right] - \lambda^2 \sigma(z) V = 0, \quad (12)$$

with the following condition on the upper boundary  $z = 0$ :

$$\sigma(0) \frac{dV}{dz} \Big|_{z=0} = 1. \quad (13)$$

By the boundary condition  $u(r, z)|_{z=H} = 0$  on the lower boundary for  $z = H$  we get:

$$V|_{z=H} = 0. \quad (14)$$

Thus, the Bessel-Fourier image  $V(\lambda, z)$  of the function  $u(r, z)$  satisfies the two-point boundary value problem (12)-(14) in the bounded interval  $[0, H]$ . Having the function  $V(\lambda, z)$  we can derive the solution of problem (1) by the following inversion formula:

$$u(r, z) = \int_0^\infty V(\lambda, z) J_0(\lambda r) \lambda d\lambda = \int_0^\infty \left( -\frac{e^{-\lambda z}}{\sigma(0)\lambda} + \bar{V}(\lambda, z) \right) J_0(\lambda r) \lambda d\lambda.$$

To define the output data  $\psi(r)$ , we use representation (8), and calculate the derivative  $\partial u(r, 0) / \partial r(r, 0)$ :

$$\frac{\partial u(r, 0)}{\partial r} = \frac{1}{\sigma(0)r^2} + \frac{\partial \bar{u}(r, 0)}{\partial r} = \frac{1}{\sigma(0)r^2} + \int_0^\infty \bar{V}(\lambda, 0) \frac{\partial J_0(\lambda r)}{\partial r} \lambda d\lambda.$$

Hence,

$$\psi(r) = \frac{\partial u(r,0)}{\partial r} = \frac{1}{\sigma(0)r^2} + \int_0^\infty \lambda \bar{V}(\lambda, 0) J_1(\lambda r) \lambda d\lambda. \quad (15)$$

Further we define the transformed output measured data

$$\varphi(\lambda) = \int_0^\infty \psi(r) J_1(\lambda r) r dr,$$

Then, according to (15) we have:

$$\varphi(\lambda) = -\frac{1}{\sigma(0)} + \int_0^\infty \bar{\psi}(r) J_1(\lambda r) r dr. \quad (16)$$

Taking into account formulas (10) and (15) we can rewrite the functional (5) in the following form:

$$J(\sigma) = \int_0^\infty (\psi(r) - \frac{\partial u}{\partial r}(r, 0; \sigma))^2 r dr = \int_0^\infty (\bar{\psi}(r) - \frac{\partial \bar{u}}{\partial r}(r, 0; \sigma))^2 r dr.$$

Thus, due to the unitary property of the Bessel-Fourier transformation, and formulas (9) and (16), the cost functional has the form:

$$J(\sigma) = \int_0^\infty (\varphi(\lambda) - \lambda V(\lambda, 0; \sigma))^2 \lambda d\lambda. \quad (17)$$

We will consider the above minimization problem for the transformed functional (17) in the set of admissible conductivity coefficients  $S$ . This set is defined as follows:

$$S := \{\sigma(z) \in C^2[0, H] : \sigma'(0) = 0, \sigma(0) = \sigma_0, \quad 0 < \sigma_1 \leq \sigma(z) \leq \sigma_2 < \infty\}. \quad (18)$$

Physically conditions  $\sigma'(0) = 0, \sigma(0) = \sigma_0$  mean that in neighborhood of the surface  $z = 0$  the conductivity of a medium is almost the constant  $\sigma_0 > 0$ . In view of functions  $p(z)$ , set of of admissible (transformed) coefficients is defined as follows:

$$P = \{p(z) \in C^1[0, H], p(z) = (\ln(\sigma(z)))', \sigma(z) \in S\}. \quad (19)$$

Now we are going to show that the transformed auxiliary functional  $\tilde{J}(p) := J(\sigma(p))$  given by (17), is a Frechet differentiable one. Note that a formula for Frechet derivative of the functional  $J(\sigma)$  has formally been given in [1], without any mathematical framework.

To prove Frechet differentiability of the transformed auxiliary functional  $\tilde{J}(p) := J(\sigma(p))$ , first we consider the following equation:

$$\frac{d^2 y}{dx^2} - \lambda^2 s^2(x) y(x) = 0, \quad (20)$$

which can be derived from equation (12) by using the following variable change

$$x(z) = \int_0^z \frac{d\zeta}{\sigma(\zeta)}, \quad x \in [0, H_1], \quad H_1 = \int_0^H \frac{d\zeta}{\sigma(\zeta)}. \quad (21)$$

Denote by  $s(x)$  the transformed conductivity function:  $s(x) := \sigma(z(x))$ . Obviously,  $0 < \sigma_1 \leq s(x) \leq \sigma_2$ . It is known that equation (20) has two fundamental solutions  $y_1(x)$  and  $y_2(x)$ . These solutions have the following asymptotics:

$$\begin{aligned} y_{1,2}(x) &= s^{-1/2} \exp(\pm \lambda z(x)) \left(1 + \frac{\varepsilon_{1,2}(x, \lambda)}{\lambda}\right), \\ |\varepsilon_{1,2}(x, \lambda)| &\leq C, \quad x \in [0, H_1], \lambda \geq \lambda_0 > 0 \end{aligned} \quad (22)$$

when  $\lambda \rightarrow \infty$  [6, 29], and the constant  $C > 0$  does not depend on  $x$  and  $\lambda$ . Differentiating the both sides of (22) we get ([6, 29]):

$$\begin{aligned} y'_{1,2}(x) &= \pm \lambda \sqrt{s} \exp(\pm \lambda z(x)) \left(1 + \frac{\varepsilon_{3,4}(x, \lambda)}{\lambda}\right), \\ |\varepsilon_{3,4}(x, \lambda)| &\leq C, \quad x \in [0, H_1], \lambda \geq \lambda_0 > 0 \end{aligned} \quad (23)$$

Further we will use the common notation  $\varepsilon(x, \lambda)$  for the above functions  $\varepsilon_{i,j}(x, \lambda)$ , since they satisfy the condition  $|\varepsilon_{i,j}(x, \lambda)| \leq C$ .

The following result is related to the estimation of the integral depending on the first variation of the solution  $V(\lambda, z; \sigma)$  of the boundary value problem (12)-(14), via the norm  $\|\delta p\|_{C^1[0, H]}$ .

**Proposition 1.** *Let  $\delta V := V(\lambda, z; \sigma + \delta\sigma) - V(\lambda, z; \sigma)$  be the first variation of the solution of the boundary value problem (12)-(14) corresponding to the admissible coefficients  $\sigma, \sigma + \delta\sigma \in S$ . Then  $\delta V$  can be estimated as follow:*

$$\left| \int_0^\infty \lambda^3 \delta V^2(\lambda, 0) d\lambda \right| \leq C(\lambda_0, H) \|\delta p\|_{C^1[0, H]}^2, \quad (24)$$

where  $\delta p \in P$  can be expressed via  $\delta\sigma \in P$  via formula (7).

**Proof.** By virtue of definition  $p(z)$  and formula (7) the variation  $\delta p(z)$  corresponds to the variation  $\delta\sigma(z)$ , that is

$$\delta\sigma(z) = \sigma(z) \cdot \int_0^z \delta p(t) dt. \quad (25)$$

Denote by  $\delta V := V(\lambda, z; \sigma + \delta\sigma) - V(\lambda, z; \sigma)$  the variation of the solution of problem (12) - (14) corresponding to the variation  $\delta\sigma(z)$ . Let us write equation (12) in variation:

$$(\delta\sigma \cdot V')' + (\sigma \cdot \delta V')' - \lambda^2(\sigma \cdot \delta V + \delta\sigma \cdot V) = 0. \quad (26)$$

Multiplying the both sides of (26) by  $(-V)$  and taking into account identities

$$-V(\delta\sigma \cdot V')' = -(V \cdot V' \cdot \delta\sigma)' + V'^2 \delta\sigma, \quad -V(\sigma \cdot \delta V')' = -(V \cdot \delta V' \cdot \sigma)' + V' \sigma \cdot \delta V',$$

we obtain

$$(V'^2 + \lambda^2 V^2) \delta\sigma - (V \cdot V' \cdot \delta\sigma)' - (V \cdot \delta V' \cdot \sigma)' + V' \sigma \cdot \delta V' + \lambda^2 \sigma V \delta V = 0.$$

Integrating this equation on  $[0, H]$ , taking into account (25), and using  $\delta\sigma(0) = 0$ , we get:

$$\int_0^H [(V'^2 + \lambda^2 V^2) \delta\sigma + \lambda^2 \sigma V \delta V + V' \sigma \cdot \delta V'] dz = 0. \quad (27)$$

Now multiplying equation (12) by  $\delta V$ , we have:  $\lambda^2 \sigma V \delta V = \sigma' V' \delta V + \sigma V'' \delta V$ . Substituting this expression into (27) and integrating we get:

$$\int_0^H [(V'^2 + \lambda^2 V^2) \delta \sigma] dz + (\sigma V' \delta V)|_{z=H} - (\sigma V' \delta V)|_{z=0} = 0.$$

Using here the boundary conditions (13)-(14) we obtain:

$$\delta V(\lambda, 0) = \int_0^H (V'^2(\lambda, z) + \lambda^2 V^2(\lambda, z)) \delta \sigma(z) dz. \quad (28)$$

Let us use now the variable change (21). Then the function  $y(x, \lambda) = V(\lambda, z(x))$  will satisfy equation (20) and the following boundary conditions:

$$y'(0, \lambda) = 1, \quad y(H_1, \lambda) = 0. \quad (29)$$

The function  $y(x, \lambda)$  satisfying equation (20) and these boundary conditions, can be expressed in explicit form as a linear combination of the fundamental solutions of equation (20). Using boundary conditions we can easily derive the following explicit asymptotic formula for  $y(x, \lambda)$ :

$$y(x, \lambda) = \frac{1}{\lambda \sqrt{s(0)} \sqrt{s(x)}} \frac{\sinh \lambda(z(x) - H)}{\cosh \lambda H} \left[ 1 + \frac{\varepsilon(x, \lambda)}{\lambda} \right]. \quad (30)$$

Note that the fulfillment of the boundary conditions (29) can be verified directly. Here  $\varepsilon(x, \lambda) \leq C$ , uniformly for  $x, \lambda$ , for enough large  $\lambda > \lambda_0$ . Taking into account the asymptotic formulas (22) and (23), we obtain:

$$\frac{dV(\lambda, z(x))}{dx} := y'(x, \lambda) = \frac{\sqrt{s(x)}}{\sqrt{s(0)}} \frac{\cosh \lambda(z(x) - H)}{\cosh \lambda H} \left[ 1 + \frac{\varepsilon(x, \lambda)}{\lambda} \right]. \quad (31)$$

Let us rewrite now the variation formula (28) in transformed form, having  $dV(\lambda, z)/dz = (1/s(x))dV(\lambda, z(x))/dx$ :

$$\delta V(\lambda, 0) = \int_0^{H_1} \left( \frac{1}{s^2(x)} y'^2(x, \lambda) + \lambda^2 y^2(x, \lambda) \right) \delta s(x) s(x) dx. \quad (32)$$

Here  $\delta s(x) = \delta \sigma(z(x))$ . Substituting in (32) expressions (30)-(31) we get:

$$\delta V(\lambda, 0) = \frac{1}{s(0)} \int_0^{H_1} \frac{\cosh^2 \lambda(z(x) - H) + \sinh^2 \lambda(z(x) - H)}{\cosh^2 \lambda H} \left[ 1 + \frac{\varepsilon(x, \lambda)}{\lambda} \right] \delta s(x) dx.$$

Hence,

$$\delta V(\lambda, 0) = \frac{2}{s(0)} \int_0^{H_1} \frac{\cosh 2\lambda(z(x) - H)}{1 + 2 \cosh 2\lambda H} \left[ 1 + \frac{\varepsilon(x, \lambda)}{\lambda} \right] \delta s(x) dx.$$

Now we return to the variable  $z$ :

$$\delta V(\lambda, 0) = \frac{2}{s(0)} \int_0^H \frac{\cosh 2\lambda(z - H)}{1 + 2 \cosh 2\lambda H} \left[ 1 + \frac{\varepsilon(z, \lambda)}{\lambda} \right] \frac{1}{\sigma(z)} \delta \sigma(z) dz.$$

Using formula (25) we can rewrite this integral in the following form:

$$\delta V(\lambda, 0) = \frac{2}{s(0)} \int_0^H \frac{\cosh 2\lambda(z-H)}{1+2\cosh 2\lambda H} \left[ 1 + \frac{\varepsilon(z, \lambda)}{\lambda} \right] \int_0^z \delta p(t) dt dz.$$

Changing the integration order we get:

$$\delta V(\lambda, 0) = \frac{2}{s(0)} \int_0^H \delta p(t) \int_t^H \frac{\cosh 2\lambda(z-H)}{1+2\cosh 2\lambda H} \left[ 1 + \frac{\varepsilon(z, \lambda)}{\lambda} \right] dz dt. \quad (33)$$

We can estimate the right hand side of (33) by using the following inequalities:

$$1 + \frac{\varepsilon(z, \lambda)}{\lambda} \leq C_1(\lambda_0), \quad \frac{\cosh 2\lambda(z-H)}{1+2\cosh 2\lambda H} \leq \frac{\cosh 2\lambda(z-H)}{\exp(2\lambda H)}.$$

We have

$$|\delta V(\lambda, 0)| \leq \frac{2C_1 \exp(-2\lambda H)}{\sigma(0)} \int_0^H |\delta p(t)| \int_t^H \cosh 2\lambda(z-H) dz dt.$$

Hence

$$|\delta V(\lambda, 0)| \leq \frac{C_1 \exp(-2\lambda H)}{2\lambda\sigma(0)} \int_0^H |\delta p(t)| \exp 2\lambda(H-t) dt \quad (34)$$

It follows from (18) that  $\delta p(0) = 0$ , which yields

$$|\delta p(t)| \leq t \|\delta p(t)\|_{C^1([0, H])}$$

Substituting this estimation into (34) we get:

$$|\delta V(\lambda, 0)| \leq \frac{C_1}{2\lambda\sigma(0)} \|\delta p(t)\|_{C^1([0, H])} \int_0^H t \exp(-2\lambda t) dt \leq \frac{C_1}{2\lambda\sigma(0)} \|\delta p(t)\|_{C^1([0, H])} \frac{1}{(2\lambda)^2}.$$

Thus

$$(\delta V(\lambda, 0))^2 \leq \frac{C_1^2}{64\lambda^6\sigma(0)^2} \|\delta p(t)\|_{C^1([0, H])}^2.$$

Multiplying the both sides by  $\lambda^3$ , where  $\lambda \geq \lambda_0$  and  $\lambda_0 > 0$  is large enough parameter, and integrating on  $[\lambda_0, \infty)$  we obtain:

$$\left| \int_{\lambda_0}^{\infty} \lambda^3 (\delta V(\lambda, 0))^2 d\lambda \right| \leq C(\lambda_0, H) \|\delta p\|_{C^1([0, H])}^2 \quad (35)$$

This implies the proof for the case  $\lambda \geq \lambda_0$ .

To prove the required estimation (24) for the case  $\lambda < \lambda_0$ , we need to show that the function  $V(\lambda, z)$  has the following property:

$$V(\lambda, z) \leq 0, \quad \forall z \in [0, H], \quad \forall \lambda \geq 0. \quad (36)$$

Indeed, multiplying the both sides of equation (12) by  $(-V)$ , integrating on  $[0, H]$ , and using the boundary conditions (13)-(14) we obtain the following energy identity

$$\int_0^H \sigma(V'^2 + \lambda^2 V^2) dz = -V(\lambda, 0). \quad (37)$$



Since the left hand side is positive, we get  $V(\lambda, 0) \leq 0, \forall \lambda \geq 0$ . Let us prove that  $V(\lambda, z) \leq 0$ , for all  $z \in (0, H]$ . We assume that there exists such a point  $z_0 \in (0, H]$  that  $V(\lambda, z_0) > 0$ . Due to the continuity of  $V(\lambda, \cdot)$ , there exists a point  $z_1 \in (0, z_0)$  such that  $V(\lambda, z_1) = 0$ . Since  $V(\lambda, H) = 0$ , the function  $V(\lambda, z)$  has a positive maximum at a some point  $z_2 \in (z_1, H)$ . As a result,  $V'(\lambda, z_2) = 0, \quad V''(\lambda, z_2) \leq 0$ . Using these conditions in equation (12) we have:

$$\lambda^2 V(\lambda, z_2) = \sigma(z_2)V''(\lambda, z_2) + \sigma'(z_2)V'(\lambda, z_2) = \sigma(z_2)V''(\lambda, z_2) \leq 0.$$

The contradiction  $V(\lambda, z_2) > 0$  shows that  $V(\lambda, z) \leq 0, \quad \forall z \in [0, H]$ .

Let us use properties (36) and (37) to estimate the function  $V(\lambda, z(x))$  on the interval  $[0, H]$ . For this aim, first we compare the function  $y(x, \lambda) := V(\lambda, z(x))$  with the linear function  $y_0(x) := x - H_1$ . The function  $y(x, \lambda)$  satisfies equation (20) with the following boundary conditions:

$$y'(0, \lambda) = 1, \quad y(H_1, \lambda) = 0. \quad (38)$$

Then, by (20) and (36) we get

$$\frac{d^2 \Delta y}{dx^2} = \lambda^2 s^2(x)y \leq 0,$$

for the difference  $\Delta y(x) = y(x, \lambda) - (x - H_1)$ . This yields

$$\frac{d\Delta y}{dx}(x) \leq \frac{d\Delta y}{dx}(0) = 0.$$

Using this inequality and the second boundary condition (38), we have

$$\Delta y = - \int_x^{H_1} \frac{d\Delta y}{dx}(x) dx \geq 0.$$

This means that  $V(z, \lambda) \geq x(z) - H_1$ . Taking into account (36) we obtain:

$$|V(\lambda, z)| = -V(\lambda, z).$$

Then the function  $V(\lambda, z)$  is estimated as follows:

$$|V(\lambda, z)| \leq H_1 - x(z) = \int_z^H \frac{dz}{\sigma(z)} \leq \frac{H}{\sigma_1}, \quad z \in [0, H]. \quad (39)$$

Now we can estimate  $\delta V(\lambda, 0)$ . Substituting the function  $\delta\sigma(z)$  from (25) into (28) and changing the integration order we get:

$$\begin{aligned} \delta V(\lambda, 0) &= \int_0^H (\sigma(z)V'^2(\lambda, z) + \lambda^2 V^2(\lambda, z))\sigma(z) \int_0^z \delta p(t) dt dz \\ &= \int_0^H \delta p(t) \int_t^H (\sigma(z)V'^2(\lambda, z) + \lambda^2 V^2(\lambda, z)) dz dt. \end{aligned}$$

Thus

$$|\delta V(\lambda, 0)| \leq \left( \int_0^H |\delta p(t)| dt \right) \int_0^H (\sigma(z)V'^2(\lambda, z) + \lambda^2 V^2(\lambda, z)) dz.$$

Taking into account identity (37) and estimation (39) we finally have

$$|\delta V(\lambda, 0)| \leq \frac{H^2}{\sigma_1} \|\delta p(t)\|_{C([0, H])} \leq C_2 \|\delta p(t)\|_{C^1([0, H])}.$$

This yields

$$\left| \int_0^{\lambda_0} \lambda^2 \delta V^2(\lambda, 0) \lambda d\lambda \right| \leq \frac{1}{4} \lambda_0^4 C_2^2 \|\delta p(t)\|_{C^1([0, H])}^2.$$

This estimate with (35) complete the proof.  $\square$

**Proposition 2.** *The functional  $\tilde{J}(p) := J(\sigma(p))$  is a Frechet differentiable one with respect to the variable  $p$  and has the following Frechet gradient:*

$$\nabla \tilde{J}[p](z) = 2 \int_0^\infty (\lambda V(\lambda, 0) - \varphi(\lambda)) \int_z^H (V'^2(\lambda, \zeta) + \lambda^2 V^2(\lambda, \zeta)) \sigma(0) \exp\left(\int_0^\zeta p(t) dt\right) d\zeta \lambda^2 d\lambda. \quad (40)$$

**Proof.** We need to show that the increment of the functional can be represented as follows:

$$\Delta \tilde{J} = \tilde{J}(p + \delta p) - \tilde{J}(p) = \langle \nabla J, \delta p \rangle + o(\|\delta p\|) = \int_0^H q(z) \delta p(z) dz + o(\|\delta p\|_{C([0, H])}), \quad (41)$$

for some function  $q(z)$ . It follows from (17) that

$$\begin{aligned} \Delta \tilde{J} &= \tilde{J}(p + \delta p) - \tilde{J}(p) \\ &= \int_0^\infty [\varphi(\lambda) - \lambda(V(\lambda, 0) + \delta V(\lambda, 0))]^2 \lambda d\lambda - \int_0^\infty (\varphi(\lambda) - \lambda V(\lambda, 0))^2 \lambda d\lambda \\ &= 2 \int_0^\infty (\lambda V(\lambda, 0) - \varphi(\lambda)) \lambda^2 \cdot \delta V(\lambda, 0) d\lambda + \int_0^\infty \lambda^2 \cdot \delta V^2(\lambda, 0) \lambda d\lambda. \end{aligned} \quad (42)$$

Substituting (28) we obtain that the linear part of (42) can be represented in the following form:

$$\delta \tilde{J} = 2 \int_0^\infty (\lambda V(\lambda, 0) - \varphi(\lambda)) \lambda^2 \int_0^H (V'^2(\lambda, z) + \lambda^2 V^2(\lambda, z)) \delta \sigma(z) dz d\lambda.$$

Thus

$$\delta \tilde{J} = 2 \int_0^H \left\{ \int_0^\infty (V'^2(\lambda, z) + \lambda^2 V^2(\lambda, z)) (\lambda V(\lambda, 0) - \varphi(\lambda)) \lambda^2 d\lambda \right\} \delta \sigma(z) dz. \quad (43)$$

Further we use the formal notation

$$\frac{\partial \tilde{J}}{\partial \sigma}(\zeta) = 2 \int_0^\infty (\lambda V(\lambda, 0) - \varphi(\lambda)) (V'^2(\lambda, \zeta) + \lambda^2 V^2(\lambda, \zeta)) \lambda^2 d\lambda \quad (44)$$

for the inner integral in the formula (43). Note that this expression coincides with the formula given in [1]. Rewrite formula (43) using (25) and changing the integration order:

$$\delta \tilde{J} = \int_0^H \frac{\partial \tilde{J}}{\partial \sigma} \cdot \sigma(\zeta) \int_0^\zeta \delta p(z) dz d\zeta = \int_0^H \int_\zeta^H \frac{\partial J}{\partial \sigma}(\zeta) \sigma(\zeta) d\zeta \delta p(z) dz.$$

Therefore the increment (42) of the functional  $\tilde{J}(p)$  can be rewritten as follow:

$$\Delta \tilde{J} = \int_0^H \int_\zeta^H \frac{\partial J}{\partial \sigma}(\zeta) \sigma(\zeta) d\zeta \delta p(z) dz + \int_0^\infty \lambda^3 \cdot \delta V^2(\lambda, 0) d\lambda. \quad (45)$$

The second term of increment (45) vanishes, when  $\|\delta p\|_{C^1([0,H])} \rightarrow 0$ , due to Proposition 1. This means that the considered functional is Frechet differentiable. Substituting here (44) and taking into account (7) and (41), we obtain the required formula (40).  $\square$

### 3. Computational experiments and their interpretation

Due to ill-posedness of the considered inverse problem, the inverse map  $\Lambda^{-1}$  is not continuous. This means that very close measured output data  $\psi(r)$  and  $\tilde{\psi}(r)$  may correspond to different conductivity coefficients  $\sigma(z)$  and  $\tilde{\sigma}(z)$ . On the other hand, iteration process of the the Conjugate Gradient Method (CGM), which is used for the numerical solution of the considered inverse problem, may not converge for any initial iteration. But, if even this process converges for some value of the conductivity ratio, an increase of this value may lead to divergence. Hence, one also needs to find out an admissible values of the conductivity coefficient  $\sigma(z)$  of media, for which the inverse problem can accurately will be solved.

This section consists of the following subsections: convergence of the iteration process depending on initial iteration and accuracy of the inverse problem solution in the case of noisy free synthetic data; noise simulation; computational results for noisy data and their interpretation.

*3.1. Convergence of the iteration process depending on initial iteration.* For the given function  $\sigma_s(z) = \exp(-9z^2) + 0.1$  the transformed direct problem was solved numerically to generate the synthetic data  $\varphi(\lambda) = \lambda V(\lambda, 0)$ . For this data the minimization problem

$$\tilde{J}(p_*) = \inf_{p \in P} \tilde{J}(p),$$

was solved by the CGM [28]. Here  $\tilde{J}(p) = J(\sigma(p))$ ,  $J(\sigma(p))$  is the transformed functional given by (17) and  $P \subset C^1[0, H]$  is the set of admissible (transformed) coefficients. Since the set of admissible coefficients is given by the values  $\sigma(0)$ , and  $\sigma'(0) = 0$  of the conductivity coefficient, in the first case the function  $\sigma_1^{(0)} = \sigma_s(0)$  was taken as an initial iteration. Convergence of the iteration process in this case was achieved at 4500 iterations. For the next initial iteration  $\sigma_1^{(0)} = 0.5(\sigma(0) + \sigma_s(z))$ , the convergence of the same iteration process was achieved at 2700 iterations. In the both cases the parameter  $\varepsilon_J > 0$  in the stopping condition  $J(p_h^{(n)}) \leq \varepsilon_J$  was taken to be  $\varepsilon_J = 10^{-6}$ . For the value  $\kappa := \sigma_2/\sigma_1 = 11$  of the conductivity ratio the obtained results, corresponding to the both cases shown, are illustrated in Figures 1 (left figure). The maximum relative error  $\varepsilon_\sigma > 0$  in values of conductivity coefficient were about 2%. For lower values  $\kappa = 5$  of the conductivity ratio, with  $\sigma_s(z) = 0.4 \exp(-9z^2) + 0.1$  the same results were obtained at 2500 iterations. However, by increasing the parameter  $\kappa$  the loss of accuracy was observed. Thus, for the value  $\kappa = 3092$  of the conductivity ratio, and the function  $\sigma_s(z) = 500 \exp(-9z^2) + 0.1$ , worse result was obtained, even for very close to the analytical solution initial iteration (right Figure 1). This, in particular, means that for high values of the parameter  $\kappa = \sigma_2/\sigma_1$  the problem became severely ill-conditioned, even in the case of noisy free data.

*3.2. Noise simulation.* To analyze the inverse problem for noisy data, first of all, one needs to simulate noisy data. It is known that (see, for example, [11]) the measured output data  $\psi(r)$  is usually generated at some discrete points of the surface  $z = 0$ . Then based on these discrete data the corresponding interpolant is constructed on the interval  $[r_{min}, r_{max}]$ ,  $r_{min} > 0$ , in logarithmic scale, where  $r_{min} \sim 0.01H_{max}$ ,  $r_{max} \sim 10H_{max}$ ,  $H_{max}$  is a desired penetration depth. During this interpolation the data  $\psi(r)$  needs to be smoothed by using high-frequency filter. Note that in practice the number of sampling points is about 20-30. To obtain noisy measured output data we assume that the measured values  $\partial u/\partial r(x_k, 0)$ ,  $k = 1, \dots, m$ , of the derivative are given on a uniform logarithmic grid with the grid points  $x_k = kh$ ,  $h = \ln(1 + r_{max})/m$ . We define the measurement error as the function  $\chi_k = \chi(x_k)$ , with continuation  $\chi_0 := \chi(x_0) = 0$ . Then the random noise can be simulated by the following Fourier sum (finite combination of harmonics):

$$\chi(x) = \sum_{k=1}^m a_k \sin\left(\frac{kx}{L}\right), \quad x = \ln(1 + r), \quad L = \ln(1 + r_{max}).$$

The coefficients  $a_k$  here are assumed to be random variables, uniformly distributed on the interval  $[-\delta_1, \delta_1]$ , where  $\delta_1 > 0$  is defined to be a noise level.

The second source of noise occurs from the value  $\sigma_0 = \sigma(0)$  of the conductivity at the surface  $z = 0$  of a medium. As it follows from formula (16) the difference  $\delta_2$  between the noisy free and noisy transformed data is the constant:

$$\delta_2 = \frac{1}{\sigma_0 + \Delta\sigma_0} - \frac{1}{\sigma_0}.$$

Therefore, the second noise can be generated by adding the constant to the transformed measured output data  $\varphi(\lambda)$ . Thus, the parameters  $\delta_1, \delta_2 > 0$  will be defined to be noise levels.

The typical noisy data  $\chi(r)$  and its Bessel transformation  $\gamma(\lambda)$  are presented on Figure 2 (left and right figures, respectively).

**3.3. Computational results for noisy data and their interpretation.** The above introduced parameters  $\delta_1, \delta_2 > 0$  do not depend on the measured output data  $\varphi(\lambda)$ . On the other hand, for real physical problem one needs to take into account the relative noisy level

$$\delta_\gamma = \max_\lambda |\gamma(\lambda) + \delta_2| / \max_\lambda |\varphi(\lambda)|, \quad (46)$$

which depends on  $\delta_1, \delta_2$  and shows actual measurement error. Computational experiments were realized for the following cases related to the conductivity function  $\sigma(z)$ :

- c1)**  $\sigma(z)$  is a monotone decreasing function;
- c2)**  $\sigma(z)$  is a monotone increasing function;
- c3)**  $\sigma(z)$  has a local minimum or maximum;
- c4)**  $\sigma(z)$  has several local minimum or maximum.

As computational experiments show, in all cases convergence of iteration process highly depends on the conductivity ratio  $\kappa$ . Further, there exists an interval for  $\kappa$ , behind which the reconstruction is unacceptable. Finally, the number of iterations  $n_i$  monotonically depends on  $\kappa$ ; specifically, this number increases by increasing the parameter  $\kappa$ .

Table 1 shows the results of computational experiments related to the cases **c1)** and **c2)**, and for various values of noise parameters  $\delta_1, \delta_2$  and  $\delta_\gamma$ .

In the first case, when  $\sigma_{\min} = \sigma_1 = 0.1$  and  $\sigma_{\max} = \sigma_2 = 1.1$ , the quality of reconstruction of  $\sigma(z)$  is high enough until the noise errors  $\delta_1 = \delta_2 = 0.1$ , and  $\delta_\gamma = 1.49\%$  (Table 1, line 3). Further increase of the noise parameters leads to the unacceptable result (line 4). Deteriorations occur, when the parameters  $\sigma_1$  and  $\sigma_2$  increase (left Figure 3). Thus for  $\sigma_1 = 0.5$  and  $\sigma_2 = 2.0$ ,  $\delta_1 = \delta_2 = 0.1$ ,  $\delta_\gamma = 9.10\%$ , the relative recovery error for  $\sigma(z)$  is about 16.22% (Table 1, line 5). For all values of noise parameters, corresponding to relative noise level  $\delta_\gamma \leq 2\%$  the iteration process converges up to the value  $10^4$  of the parameter  $\kappa$ .

In all cases the iterations process was stopped when the auxiliary function became significantly less then the noise level, namely, when  $\max |\lambda V(\lambda, 0) - \varphi(\lambda)| \simeq 0.1 \max |\gamma(\lambda) + \delta_2|$ .

Consider now the case **c2)**. Here we compared an influences of the different noise levels  $\delta_1, \delta_2$  on computational results. It is clear from Table 1 that the influence of the parameter  $\delta_2$  on the reconstruction quality is significantly higher, than the influence of  $\delta_1$ . For example, for  $\delta_1 = 0, \delta_2 = -0.01$ , the relative reconstruction error is about 45.6% (Table 1, line 11), whereas for  $\delta_1 = 0.01, \delta_2 = 0$ , this error is 5.85% (line 9). Right figure 3 displays the reconstruction of the coefficient  $\sigma(z)$  for these cases. It follows from lines 13 and 14 of Table 1 that further increase of the noise level  $|\delta_2|$  leads to unacceptable results. Unlike the case **c1)**, in the case of a monotone increasing  $\sigma(z)$ , reconstruction was found to be possible in the interval  $[1, 30]$  of the conductivity ratio  $\kappa$  (left Figure 4). Observe that a further increase of the parameter  $\kappa$  increases the degree of ill-conditionedness of the inverse problem.

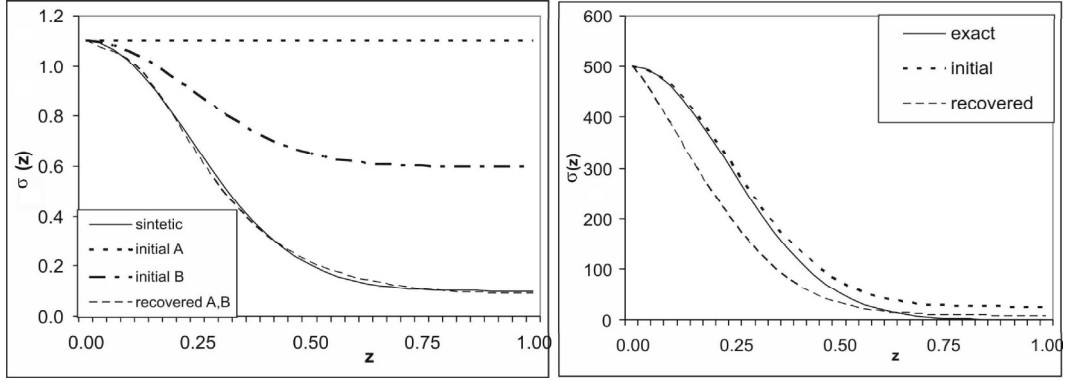


Figure 1: Reconstruction of the function  $\sigma(z) = a \exp(-9z^2) + 0.1$  with different initial iterations and conductivity ratios:  $a = 1, \kappa = 11$  (left figure),  $a = 500, \kappa = 3092$  (right figure).

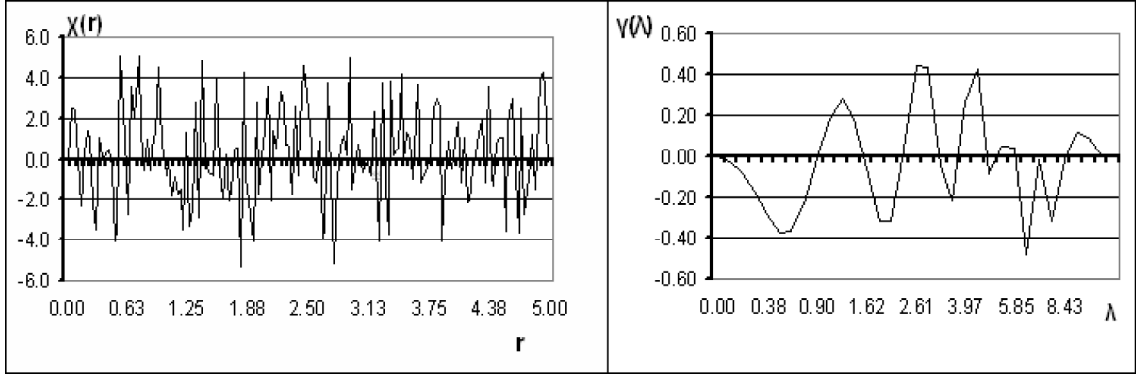


Figure 2: The typical noisy distribution (left figure) and its Bessel transformation (right figure).

Thus, for  $\kappa = 500$ , the relative reconstruction error is about 50%, even in the case, when the initial iteration is chosen to be very close to the exact solution. Hence, for such values of the parameter  $\kappa$ , two output data, which are quite close to each other, may correspond to very different conductivity functions (right Figure 4).

The case  $\kappa = 500$  also led to instability. Different reconstructed coefficients were obtained for different initial iterations, in the case when the conductivity function was drastically increasing with the depth. Figure 5 displays two numerical examples corresponding to this case. A satisfactory result was obtained when the initial guess was monotonically increasing function (right Figure 5). For the value  $\varepsilon_J = 10^{-9}$  of the stopping parameter the relative error  $\sigma(z)$  19% was achieved at 150000 iterations. However, in the case of wave-like function as an initial iteration, to obtain a satisfactory resolution was unable, even at 700000 iterations and  $\varepsilon_J = 10^{-8}$ , as the left Figure 5 shows. The stopping parameter for the gradient method in this case was taken to be  $10^{-12}$ .

The above obtained computational results have precise physical meaning. When the conductivity is increasing with the depth, layers with the larger resistance are located above the layers with smaller resistance. Hence, top layers overshadow lower ones. This means that the impact of lower layers in the output data on the surface is too small to be noticed. It is natural therefore that the residual functional is not sensitive to variations of the conductivity of lower layers.

Acceptable results are obtained also for the cases **c3)**-**c4)**. As in the cases **c1)**-**c2)**, the algorithm

Table 1: Relative errors for different noise level

cases	No	$\delta_1$	$\delta_2$	relative noise level ( $\delta_\gamma$ )	relative reconstruction error (for $\sigma(z)$ )
c1) $\sigma_1 = 0.1,$ $\sigma_2 = 1.1$	1	0	0	0.0%	2.44%
	2	0.01	0.01	0.18%	2.36%
	3	0.1	0.1	1.49%	9.09%
	4	0.2	0.2	4.82%	26.52%
c1) $\sigma_1 = 0.5,$ $\sigma_2 = 2.0$	5	0.1	0.1	9.10%	16.22%
c2), monotone increasing $\sigma(z)$	6	0	0	0.0%	2.00%
	7	0.001	0.001	0.24%	2.27%
	8	0.005	0.005	1.19%	15.13%
	9	0.01	0	0.17%	5.85%
	10	0	0.01	2.35%	31.01%
	11	0	-0.01	2.12%	45.60%
	12	0.05	0	0.86%	34.31%
	13	0	0.05	9.93%	55.24%
	14	0	-0.05	12.77%	494.02%

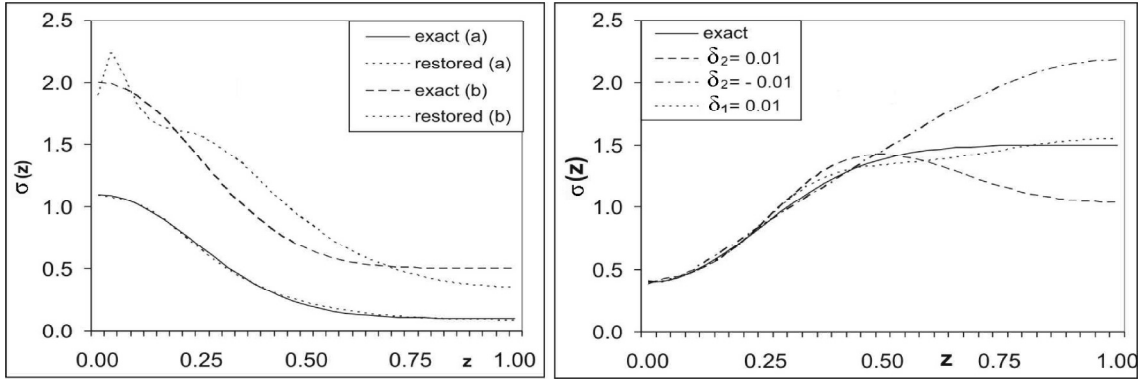


Figure 3: The comparison of recovered data with different  $\sigma(z)$  distribution (left figure) and with different noise level (right figure).

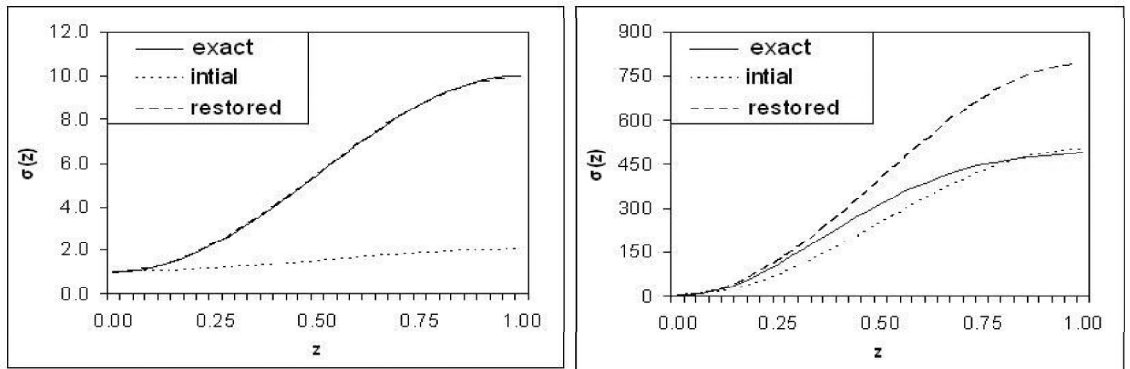


Figure 4: The recovery of the monotone function  $\sigma(z)$  corresponding to values of the ratio  $\sigma_2/\sigma_1 = 1 \cdot 10^1$  (left figure) and  $\sigma_2/\sigma_1 = 5 \cdot 10^2$  (right figure).

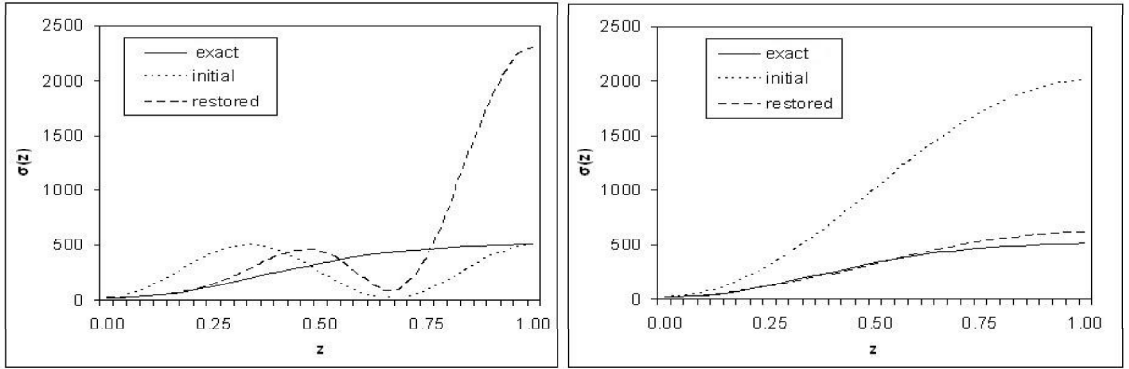


Figure 5: The comparison between recovered data for different initial iterations for conductivity ratio  $\kappa = 500$ .

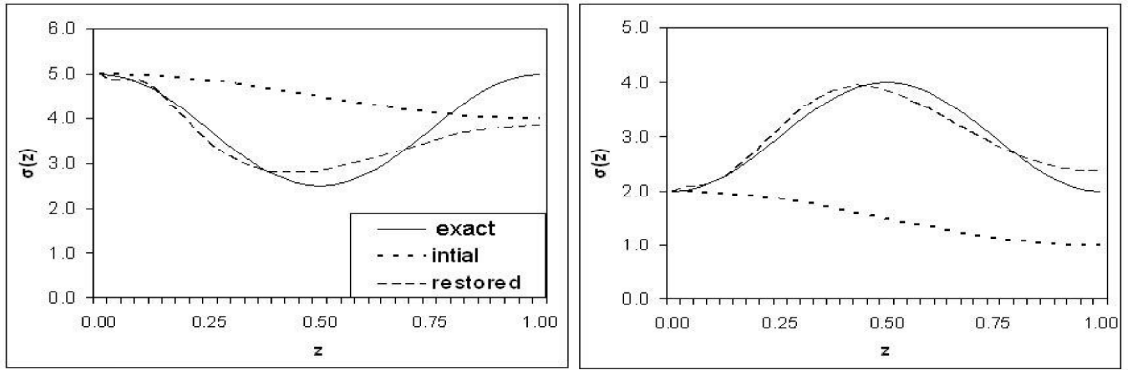


Figure 6: The recovered coefficient  $\sigma(z)$  with extreme points: minimum ( $\sigma_2/\sigma_1 = 2$ ) and maximum ( $\sigma_2/\sigma_1 = 10$ ).

performs better when the contrast of the medium decreases, which corresponds to lower values of the conductivity ratio  $\kappa$ . Similarly, the iteration process diverges for large values of  $\kappa$ .

In the case **c3**), an admissible result is obtained also for the conductivity function having a local minimum, when  $\kappa \leq 0.5 \cdot 10^1$ . For the conductivity function with local maximum, this ratio can be increased until  $\kappa \leq 3 \cdot 10^1$  (Figure 6).

The cases when the layers with the minimal conductivity are located far from the measurement surface, were also unfavorable. The reason of this phenomenon is that, in this case we have an analogue the same effect of "overshadowing" described above. Indeed, in this case layers with low conductivity are located above the ones with higher conductivity. Hence, the current simply almost does not reach lower layers.

We have obtained correct result until the layers with the minimal conductivity, whereas the recovery quality for lower layers was strongly decreasing (Figure 6).

Finally consider the case **c4**). Accurate results were obtained in the layers nearest to the surface, and the function  $\sigma(z)$  was recovered even for the rough initial iteration (Figure 7). However, in the case of larger depths, the values of the  $\sigma(z)$  moved away from the exact solution, even for the value  $\kappa \approx 6.0$  of the conductivity ratio, although the values of the cost functional were decreasing, by increasing the number of iterations. Acceptable results were obtained for the values  $\kappa \leq 5.0$ . The solution of the

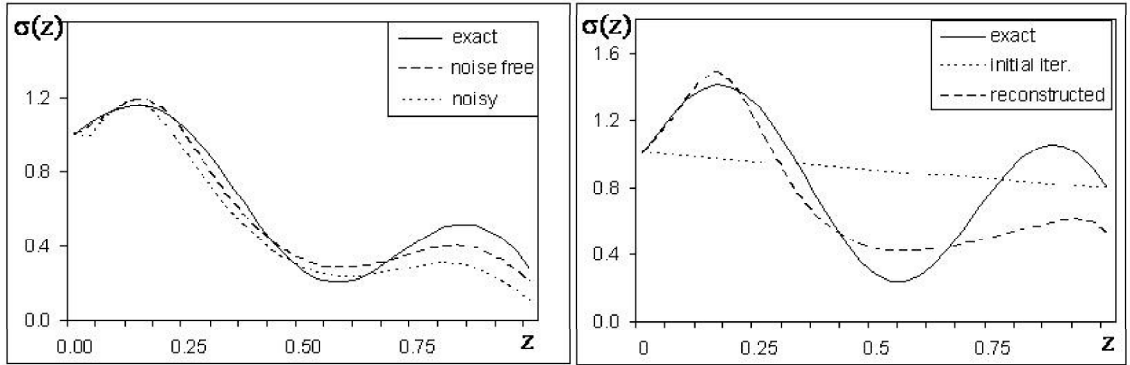


Figure 7: The recovery of the wave-like coefficient  $\sigma(z)$  with different ratio ( $\sigma_2/\sigma_1 = 0.5 \cdot 10^1$ ) (left figure) and ( $\sigma_2/\sigma_1 = 0.6 \cdot 10^1$ ) (right figure).

inverse problem, corresponding to this case, is shown on the left Figure 7. The presented here results include noise free data and the noisy data with the noise levels  $\delta_2 = 0$ ,  $\delta_1 = 1 \cdot 10^{-1}$ .

Thus for the medium with continuous conductivity function the analogue of the equivalence principle (see, Appendix) is also observed. In particular, this phenomenon takes place for an increasing function  $\sigma(z)$  as well as for the case of minimal conductivity at large depth. It turns out that very close output information (2) of the problem (1)-(2) can correspond to different conductivity distributions, especially for the large conductivity ratio  $\kappa$ .

#### 4. Conclusions

The goal of this paper is to construct a numerical method for the recovery of the unknown conductivity coefficient in the inverse resistivity problem. The mathematical model based on the transformed measured data is proposed. The method is implemented numerically for various realistic values of physical parameters of a layered medium. Computational results with noisy free and noise data demonstrate that for some realistic conductivity values the unknown coefficient can be reconstructed with enough accuracy.

#### Acknowledgements

The authors thank Alemdar Hasanoglu (Hasanov) for valuable suggestions which improved the manuscript. The authors also thank anonymous referees for constructive criticism. This work was supported by Ministry of Education and Research of Kazakhstan under the Grant No 0102RK00232

#### References

- [1] Alekseev A.S., Tcheverda, V.A., Niambaa Sh. Optimizational method for solving the inverse problem of geophysical prospecting by electric means under direct current for vertically-inhomogeneous media. Inverse Modelling in Exploration Geophysics. Braunschweig, Wiesbaden, (1989) 171-189.
- [2] A. M. Bruaset, A Survey of Preconditioned Iterative Methods, New York: Addison-Wesley, 1995.
- [3] A.P. Calderon. On an inverse boundary value problems. Seminar on Numerical Analysis and its Applications to Continuum Physics (Society Brasileira de Matematica), 1980) 65-73.
- [4] M. Cheney, D. Isaacson, J.S. Newell, Electrical impedance tomography, SIAM Review, 41(1999), 85-101.



- [5] D. Colton and R. Kress, Integral equation methods in scattering theory, Wiley, New York, 1983
- [6] M.A. Evgrafov, M.V. Fedoriuk, Asymptotics of solutions of the equation  $w''(x) - p(z, \lambda)w = 0$  solutions in the complex plane  $z$ , under the condition  $\lambda \rightarrow +\infty$ , Russian Mathematical Surveys, 21(1966) 3-50(in Russian).
- [7] A. Hasanov, Inverse coefficient problems for monotone potential operators, Inverse Problems, 13(1997), 1265-1278.
- [8] A. Hasanov, P. DuChateau, B. Pektas, An adjoint problem approach and coarse-fine mesh method for identification of the diffusion coefficient in a linear parabolic equation, Journal of Inverse and Ill-Posed Problems, 14(2006), 1-29.
- [9] O. Koefoed, The Application of the Kernel Function in Interpreting Geoelectrical Resistivity Measurements. Berlin: Borntrager, 1968.
- [10] O. Koefoed, Error propagation and uncertainty in the interpretation of resistivity sounding data, Geophysical Prospecting, Volume 24/1(1976) 31-48.
- [11] O. Koefoed, Geosounding Principles: Resistivity Sounding Measurements. Hardcover, Elsevier, 1979
- [12] V.V. Kuskov, Numerical modelling of vertical electrical sounding in two dimensional inhomogeneous medium. Vestnik MGU, Ser.4-Geology, 1(1985) 82-88 (in Russian).
- [13] S. Narayant, M.B. Dusseault and D. C. Nobes. Inversion techniques applied to resistivity inverse problems, Inverse Problems, 10(1994) 669-686.
- [14] S.Niwas, Olivar A.L. de Lima, Unified equation for straightforward inversion scheme on vertical electrical sounding data. Geofizika. 23/1(2006) 22-33.
- [15] M. Orunkhanov, B. Mukanova, B.Sarbasova, Convergence of the method of integral equations for quasi three-dimensional problem of electrical sounding, In Proc. Computational Science and High Performance Computing II (The Second Advanced Research Workshop, Stuttgart, Germany, March 14-16, 2005), Germany: Springer, 2005.
- [16] M. Orunkhanov and B. Mukanova. The integral equations method in problems of electrical sounding, Proc. Advances in High Performance Computing and Computational Sciences. 93(2006) 15-21, Berlin/Heidelberg: Springer.
- [17] W.H. Pelton, L. Rijo and C.M. Swift(Jr.) Inversion of two dimensional resistivity and induced polarization data, Geophysics, 43(1978) 788-803.
- [18] P.A.T. Pinheiro, W.W. Loh and F.J. Dickin. Smoothness-constrained inversion for two-dimensional electrical resistance tomography. Meas. Sci. Technol. 8(1997) 293-302.
- [19] S. Siltanen, J. Mueller, D. Isaacson, An implementation of the reconstruction of A Nachman for the 2D inverse conductivity problem, Inverse Problems, 16(2000), 681-699.
- [20] L.B. Slihter, The interpretation of resistivity prospecting method for horizontal structures, Physics, 4(1933) 307-322.
- [21] S.S. Stefanescu, C. Shlumberger, Sur la distribution électrique potentielle dans une terrain a couches horizontales, homogènes et isotropes, J. Phys. Radium, 7(1930) 132-141.
- [22] A.F. Stevenson, On the theoretical determination of earth resistance from surface potential measurements, Physics, 5(1934) 114-124.
- [23] A.N. Tikhonov, On electrical sounding above inclined bed, Proc. of Institute of Theor. Geophys. 1(1946) 116-136, Moscow-Leningrad: USSR Acad. Sci. Publ. House (in Russian).
- [24] A.N. Tikhonov, About uniqueness of geoelectrics problem solution, Doklady Acad. Sci. USSR, 69/6(1949) 797-800 (in Russian).

- [25] A.N. Tikhonov, About definiton of electrical characteristics of the earth's crust profound layers, Doklady Acad. Sci. USSR, 73/2(1950) 295-298 (in Russian).
- [26] A. Tikhonov and A. Samarskii, Equations of Mathematical Physics, London: Pergamon Press, 1963.
- [27] A. Tikhonov and V. Arsenin, Solution of Ill-Posed Problems, New York: John Wiley, 1977.
- [28] F.P. Vasil'ev, Methods for Solving Extremal Problems, Moscow: Nauka, 1981.
- [29] W. Wasov, Asymptotic Expressions for Ordinary Differential Equations, New York: John Wiley & Sons, 1965.

### Appendix. An influence of the reflection coefficient to the output data

In this section we provide some explanations related to the reason of introducing the reflection factor function  $p(z) = (\ln(\sigma(z)))'$ .

In our earlier publications [15,16] we have considered the VES-direct problem. This problem was concerned with the case when the surrounding medium, with the constant conductivity  $\sigma_1 > 0$ , contains a homogeneous subregion  $\Omega_0$ , with the conductivity  $\sigma_2 > 0$ . The corresponding mathematical problem has been formulated as follows: Find output data

$$\frac{\partial u}{\partial r}|_{z=0} = \psi(r), \quad (47)$$

via the solution of the boundary value problem

$$\left\{ \begin{array}{l} \Delta u(M) = 0, \quad M = (x, y, z) \in \Omega_0 \cup \Omega_1, \\ \Omega_0 \subset \{(x, y, z) | z > 0\} \subset R^3, \Omega_1 = \{R^3 \setminus \bar{\Omega}_0\} \cap \{z > 0\}, \\ \sigma_1 \frac{\partial u}{\partial z}|_{z=0} = \frac{1}{2\pi} \delta(r), \quad r = \sqrt{x^2 + y^2} \\ u|_{\partial\Omega_0^-} = u|_{\partial\Omega_0^+}, \quad \sigma_1 \frac{\partial u}{\partial n} \Big|_{\partial\Omega_0^-} = \sigma_2 \frac{\partial u}{\partial n} \Big|_{\partial\Omega_0^+}, \\ \lim_{\sqrt{x^2+y^2+z^2} \rightarrow \infty} u(M) = 0. \end{array} \right. \quad (48)$$

The cross-section of the domain  $\Omega_0$  with plane  $y = const$  not depends on  $y$  and it is a starshaped surface in  $\{(x, z) \in R^2, z > 0\}$ , with a smooth boundary. The model (48) describe the distribution of the electrical potential  $u(x, y, z)$  on the surface of a medium with piecewise constant conductivity.

An integral equation for an inclined plane bed has been obtained by Tikhonov in [23]. He has proposed an iterative method for the solution of this integral equation and has proved convergence of iterations. In [15-16] this method was developed for two- and three-dimensional cases. Specifically, in the case of the non-homogeneous medium with the piecewise constant conductivity, the direct problem can be modeled by the following integral equation:

$$\nu(M) = \frac{\mu}{2\pi} \int \int_{\Gamma} \nu(M_1) \frac{\partial}{\partial n} \left( \frac{1}{r_{MM_1}} + \frac{1}{r_{MM'_1}} \right) d\Gamma(M_1) + \mu F_0(M). \quad (49)$$

The parameter  $\mu = (\sigma_1 - \sigma_2)/(\sigma_1 + \sigma_2)$  has been defined to be the *reflection coefficient* (or the reflection factor) at the transmission boundary between the inclusion and the surrounding medium. Further it was shown that the function  $\nu(M)$  is the density of the simple layer potential:

$$u(P) = \frac{1}{2\pi\sigma_1} \int \int_{\Gamma} \nu(M) \left[ \frac{1}{r_{PM}} + \frac{1}{r_{PM'}} \right] d\Gamma(M). \quad (50)$$

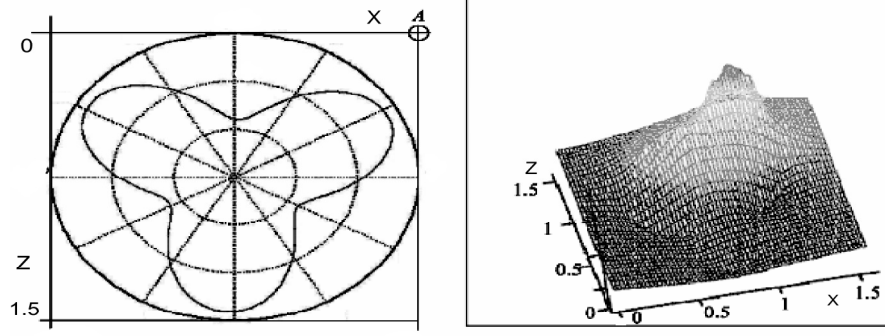


Figure 8: Geometry of the cross-section of inclusion (left figure), and cross-section of the distribution of the electrical potential  $u(M)$  at  $y=0$  (right figure).

Here  $\Gamma := \partial\Omega_0$  is the boundary of the homogeneous inclusion,  $F_0(M)$  is a given function,  $r_{MM_1}$  is the distance between the points  $M$  and  $M_1$ . The point  $M'_1$  is the reflection of the point  $M_1 \in \Gamma$  to the half space  $\{z < 0\}$ . Differentiation in the integral equation (6) is taken in the direction of the outward normal  $n$  to the surface  $\Gamma$  at the point  $M$ .

Note, that the integral equation method [5] is a very effective one for solving direct problems for stationary electromagnetic fields in homogenous media. The numerical method proposed in [15] is based on the solution of the integral equation (49) by an iterative algorithm with the follow up calculation of the function  $u(P)$  by the formula (50). The simplicity and effectiveness of this method led to small computational times. Although estimates of [15] require some bounds with respect to geometry of the inclusion, computational experiments have demonstrated that these bounds can be weakened in practice.

To analyze an influence of the reflection coefficient  $\mu$  to the output data, we apply the algorithm given in [15] to to equations (49)-(50). As a stopping criteria we use the relative error

$$\varepsilon_1 := \frac{\|u^{(n)} - u^{(n+1)}\|_{C(\Gamma)}}{\|u^{(n)}\|_{C(\Gamma)}},$$

between two consecutive iterations. 20 iterations were sufficient to achieve the accuracy  $\varepsilon_1 < 10^{-9}$ . The left Figure 8 illustrates the cross-section of the inclusion, given analytically by the function  $r(\theta) = 1.8 + 0.4\sin(3\theta + \pi/8)$ , in polar coordinates. The cross-section of the numerically computed function  $u(x, 0, z)$  is shown in the right Figure 8.

The computational experiments show that for sufficiently small values of  $\sigma_2/\sigma_1 \ll 1$  as well as for sufficiently high values  $\sigma_2/\sigma_1 \gg 1$  of the conductivity ratio, the output data given by (47) is not sensitive with respect to perturbations of the parameter  $\sigma_2$ . Therefore, in this case the inverse problem is severely ill-conditioned one.

To explain this phenomenon, we consider next example for the inclusion which geometry is given in the left Figure 8. For this aim we introduce the apparent resistivity  $r^2\partial u/\partial r$ , following to [11], as the output measured data multiplied to  $r^2$ . Further, we rewrite the reflection coefficient  $\mu = (\sigma_1 - \sigma_2)/(\sigma_1 + \sigma_2)$  in terms of the above ratio  $\kappa = \sigma_2/\sigma_1$ , as follows  $\mu = (1 - \kappa)/(1 + \kappa)$ . Evidently,  $\mu \in (-1, 1]$ . The upper and lower lines 6 and 1 in Figure 9 correspond to the used minimal and maximal values of the ratio  $\kappa$ . As show computational experiments increase or decrease of the ratio  $\kappa$  did not make the apparent resistivity lines outside of the lines 6 or 1. These lines we will defined as an *upper and lower (apparent resistivity) limit lines*, respectively, and the area between these lines will be defined as an *distinguishability domain* for the unknown coefficient  $\sigma_2$ . Based on these results

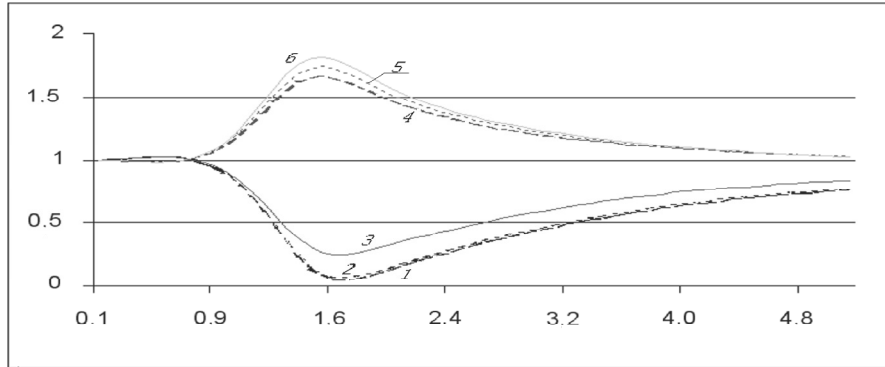


Figure 9: Output data (apparent resistivities) corresponding to different values of the ratio  $\sigma_2/\sigma_1$ : 1 –  $5 \times 10^2$ ; 2 –  $1 \times 10^2$ ; 3 –  $1 \times 10^1$ ; 4 –  $1 \times 10^{-1}$ ; 5 –  $1 \times 10^{-2}$ ; 6 –  $2 \times 10^{-3}$

we can assert that, in the case of piecewise constant medium the measured output data  $\psi(r)$  may distinguish the unknown conductivity  $\sigma_2$  only if the ratio  $\kappa$  belong to  $[2 \times 10^{-3}, 5 \times 10^2]$ , i.e. from the distinguishability domain. Further computational experiments show that distinguishability domain depends also on the distance between the inclusion and the surface.

Thus we can conclude that in the neighborhood of the upper and lower limit lines, i.e. along the boundary of the distinguishability domain, inclusions with different conductivities  $\sigma_2$  can not be distinguished by output data. In the geophysical sciences similar analogue of this phenomenon for layered media is defined to be *the principle of equivalency* ([9-11]). Hence, we can expect that the recovery of the reflection factor  $\mu$  can be more admissible, than the direct reconstruction of the  $\sigma_2$ . This is the main reason why we transformed the original inverse problem (1)-(2) to the problem of recovering the above introduced reflection factor function  $p(z) = (\ln(\sigma(z)))'$ .